BJR

https://doi.org/10.1259/bjr.20180909

Received: 20 October 2018 | Revised: 18 August 2019 | Accepted: 21 August 2019

Cite this article as:
Tang H, Liu Z, Hu Z, He T, Li D, Yu N, et al. Clinical value of a new generation adaptive statistical iterative reconstruction (ASIR-V) in the diagnosis of pulmonary nodule in low-dose chest CT. *Br J Radiol* 2019; **92**: 20180909.

FULL PAPER

Clinical value of a new generation adaptive statistical iterative reconstruction (ASIR-V) in the diagnosis of pulmonary nodule in low-dose chest CT

[1]HUI TANG, [2]ZHENTANG LIU, [2]ZHIJUN HU, [3]TAIPING HE, [2]DOU LI, [3]NAN YU, [3]YONGJUN JIA and [1]HONG SHI

[1]Department of Radiology, Xi'an No.1 Hospital, Xi'an, Shaanxi, China
[2]Department of Radiology, Chang'an Hospital, Xi'an, Shaanxi, China
[3]Department of Radiology, Affiliated Hospital of Shaanxi University of Chinese Medicine, Xianyang, Shaanxi, China

Address correspondence to: Mr Hong Shi
E-mail: *shihongkeyan@163.com*

Objective: To evaluate the clinical value of low-dose chest CT combined with the new generation adaptive statistical iterative reconstruction (ASIR-V) algorithm in the diagnosis of pulmonary nodule.

Methods: 30 patients with pulmonary nodules underwent chest CT using Revolution CT. The patients were first scanned with standard-dose at a noise index (NI) of 14, and the images were reconstructed with filtered back projection (FBP) algorithm. If pulmonary nodules were found, a low-dose targeted scan, with NI of 24, was performed localized on the nodules, and the images were reconstructed with 60% ASIR-V. The detection rate of pulmonary nodules in the two scanning modes was recorded. The size of nodules, CT value and standard deviation of nodules were measured. The signal-to-noise ratio and contrast-to-noise ratio were also calculated. Two experienced radiologists used a 5-point method to score the image quality. The volumetric CT dose index, and dose–length product were recorded and the effective dose (ED) was calculated of the two scanning modes.

Results: Volumetric CT dose index (ED) of the standard-dose scan covering the entire lungs was 7.29 ± 2.38 mGy (3.52 ± 1.09 mSv), and that of low-dose targeted scan was 2.56 ± 1.87 mGy (0.51 ± 0.32 mSv). However, the ED of the virtual low-dose scan for the entire lungs was 1.44 ± 0.15 mSv, which would mean a dose reduction of 59.1% compared with the standard-dose scan. 85 of the 87 pulmonary nodules were detected in the low-dose targeted scan, with 2 of the ground-glass density nodules with size less than 1 cm missed, resulting in 97.7% overall detection rate. There was no difference between the low-dose ASIR-V images and standard-dose FBP images for the size (1.49 ± 0.74 cm *vs* 1.48 ± 0.75 cm), CT value [33.02 ± 1.95 Hounsfield unit (HU) *vs* 34.6 ± 3.07 HU], standard deviation (27.64 ± 14.42 HU *vs* 30.38 ± 20.04 HU), signal-to-noise ratio (1.44 ± 0.88 *vs* 1.43 ± 1.31) and contrast-to-noise ratio (38.95 ± 18.43 *vs* 38.23 ± 14.99) of nodules (all $p > 0.05$). There was no difference in the subjective scores between the two scanning modes.

Conclusion: The low-dose CT scan combined with ASIR-V algorithm is of comparable value in the detection and the display of pulmonary nodules when compared with the FBP images obtained by standard-dose scan.

Advances in knowledge: This is a clinical study to evaluate the clinical value of pulmonary nodules using ASIR-V algorithm in the same patients in the low-dose chest CT scans. It suggests that ASIR-V provides similar image quality and detection rate for pulmonary nodules at much reduced radiation dose.

INTRODUCTION

Lung cancer is the most common malignant tumor with the highest morbidity and mortality in the respiratory system. Related studies[1,2] have shown that the 5-year average survival rate of patients with lung cancer (small cell lung cancer and non-small cell lung cancer) is 13–15%. While, 5-year survival rate of patients with Stage I lung cancer is as high as 70%. Pulmonary nodules, as an important manifestation of early stage lung cancer, are mainly characterized by round or irregular lesions with a diameter of no more than 3 cm in the lung, which are of great significance for the early detection and diagnosis of lung cancer. At present, the differential diagnosis of benign and malignant pulmonary nodules depends mainly on regular CT review and study of nodular multiplication relationship. The potential downside of radiation dose in CT has drawn increasing attention. Some studies[3] have shown that the radiation-related cancer risk has increased from 0.4% to 1.5–2.0% due to a

Table 1. Subjective scoring for the whole image quality

Grading score	Qualitative image analysis		
	Morphological display of all nodules	Visibility for surrounding lung tissue	Artifacts and diagnostic confidence
1	Very poor display, unclear edge	Unacceptable visibility, cannot distinguish small structures	Severe artifacts, without diagnostic confidence
2	Poor display, fuzzy edge	Small structures are not displayed very well, seriously impact diagnosis	Substantial artifacts, insufficient confidence
3	Moderate display, not very clear edge	Small structures can be displayed, and enough for diagnosis	Moderate artifacts, low confidence but diagnosis possible
4	Better display, still clear edge	Small structures can be clearly displayed with good contrast	Minor artifacts, good diagnostic confidence
5	Excellent display, clear edge	Small structures can be clearly displayed with excellent contrast	No artifacts, excellent diagnostic confidence

substantial increase in the CT examination. Patients undergoing a standard-dose chest CT scan receive 10–100 times radiation dose than that of conventional chest radiographs, especially for the high-risk groups.[4] The great radiation exposure of CT examination makes it to become the main source of iatrogenic radiation.

Low-dose chest CT scan has been used more frequently in the early lung cancer screening in clinical application.[5] The inherent high contrast and resolution, between the lung lesions and lung tissue, provide a basis for the chest low-dose CT screening of lung cancers. However, for routine CT, reducing the radiation dose will inevitably reduce the image quality, affecting the clinicians' diagnosis of pulmonary nodules. Therefore, it is important to balance between the radiation dose and image quality.

In order to obtain acceptable image quality with the minimum radiation dose, different reconstruction algorithms came into being. Compared with the traditional filtered back projection (FBP) technique, the iterative reconstruction technique can significantly reduce the image noise and provide more possibilities for reducing the radiation dose.[6] At the same time, iterative reconstruction technique, because of its real noise reduction ability to restore the scan objects, has become the focus and hotspot of many scholars. Adaptivestatistical iterative reconstruction (ASIR-V) is a new generation adaptive statistical iterative reconstruction algorithm that contains more advanced noise modeling and object modeling than the previous iterative reconstruction algorithms. ASIR-V has also added some physics modeling to be more robust in terms of reducing the image noise and improving the spatial resolution through changing the ASIR-V percentage weight.[7–10] However, there are a relatively small number of studies on ASIR-V currently, especially in the diagnosis of pulmonary nodules.

Table 2. Subjective scoring for the special morphological signs of the partial pulmonary nodules

Grading score	Qualitative image analysis for the partial pulmonary nodules
1	Very poor display for the morphologic signs, unclearly margins of the nodules
2	Poor display for the morphologic signs, fuzzy margins of the nodules
3	Moderate display for the morphologic signs, not very clearly margins of the nodules
4	Better display for the morphologic signs, still clearly margins of the nodules
5	Excellent display for the morphologic signs, very clearly margins of the nodules

This study aimed to discuss the clinical value of ASIR-V on image noise reduction and image quality improvement at reduced radiation dose in comparison with FBP technique at standard dose in the diagnosis of pulmonary nodules.

SUBJECTS AND METHODS

This study was approved by the Ethics Committees of Xi'an No.1 Hospital. All patients had signed the written informed consent.

Patient population

From January 12 to July 28, 2017, 37 patients with pulmonary nodules who were reviewed for CT examination within 3 months were initially recruited to our study. The inclusion criteria were as follows: (1) patients with pulmonary nodules less than 3 cm in diameter, (2) patients aged 18–80 years old, (3) patients with a body mass index (BMI) of 18.5–32 kg/m^2, (4) patients with complete clinical information. The exclusion criteria were as follows: (1) patients with severe respiratory symptoms who could not complete CT examination, (2) images of the patients had large artifacts caused by improper movement during the scan, (3) image quality was too poor for accurate data measurements, (4) patients with calcified pulmonary nodules.

37 patients were initially being considered with 7 patients excluded (4 patients with large image artifacts and three patients with calcified pulmonary nodules) according to the above criteria. Finally, 30 patients were included in our study including 16 males and 14 females (age range, 24–73 years; mean age, 52.86 ± 1.93 years; BMI, 22.48 ± 3.19 kg/m^2).

Table 3. Comparison of detection numbers of pulmonary nodules in the two scanning modes

Different pulmonary nodules	Standard-dose scan	Low-dose scan	Detection rate
Ground-glass density nodules	**14**	**12**	**85.71%**
Average diameter <1 cm	8	6	75%
1 cm < average diameter <2 cm	6	6	100%
2 cm < average diameter <3 cm	0	0	0
Mixed-density nodules	**18**	**18**	**100%**
Average diameter <1 cm	4	4	100%
1cm < average diameter <2 cm	9	9	100%
2cm < average diameter <3 cm	5	5	100%
Solid nodules	**55**	**55**	**100%**
Average diameter <1 cm	18	18	100%
1 cm < average diameter <2 cm	23	23	100%
2 cm < average diameter <3 cm	14	14	100%
Total number of all nodules	**87**	**85**	**97.70%**

Scanning techniques and image reconstruction

All patients underwent plain chest CT on a Revolution CT (GE Healthcare, Waukesha, WI). Patients were trained to hold breath before CT scan to minimize respiratory motion. The patients were scanned on a supine position during the examination from the apex to the top of the diaphragm with their upper arms over the head, and the images were captured at the end of inspiration. The scan parameters were as follows: tube voltage of 120 kVp, automatic tube current modulation for achieving a set noise index (NI), pitch of 0.992:1, rotation speed of 0.5 s, and image slice thickness of 5 mm. For the 30 patients, in their first visit, the chest CT images were acquired with standard dose scan (NI = 14), and reconstructed with FBP technique. If pulmonary nodules were found, a low-dose target scan, with the noise index of 24, was performed localized on the nodules on the same day, and the images were reconstructed with 60% ASIR-V algorithm. All reconstruction images included mediastinum window and lung window images, with slice thickness of 0.625 mm.

Objective image quality analysis

All images were transferred to and reviewed on an AW4.6 CT workstation with all patient, scan and reconstruction information removed. The window width of 350 Hounsfield unit (HU) and window level of 40 HU was used for the mediastinal window, and window width of 1500 HU and window level of −800 HU was used for the lung window. On the cross-sectional lung window images of the two scanning modes, the number and the type of all pulmonary nodules (ground-glass density nodule, mixed-density nodule and solid nodule) were recorded. The morphological characteristics of the pulmonary nodules (lobular sign, burr or spinous, pleural traction sign, vacuoles or voids) were also recorded for the two scanning modes. The size of all nodules, including the longest diameter, the shortest diameter, and the average diameter were measured. In addition, a circular region of interest (ROI) was placed on the nodule and the surrounding normal lung tissue area in the maximum transverse section of the nodule. The size of the ROI was consistent and placed on

Table 4. Comparison of objective results of the pulmonary nodules and surrounding normal lung tissue of the two scanning modes

Parameters	Standard-dose scan	Low-dose scan	T value	*p* value
The longest diameter of nodules (cm)	1.72 ± 0.88	1.76 ± 8.55	0.093	0.648
The shortest diameter of nodules (cm)	1.24 ± 0.69	1.23 ± 0.69	0.007	0.701
Average diameter of nodules (cm)	1.48 ± 0.75	1.49 ± 0.74	0.018	0.759
CT values of nodules (HU)	34.6 ± 3.07	33.02 ± 1.95	1.445	0.577
SD values of nodules (HU)	30.38 ± 20.04	27.64 ± 14.42	0.226	0.105
SNR values of nodules	1.43 ± 1.31	1.44 ± 0.88	2.475	0.144
CNR values of nodules	38.23 ± 14.99	38.95 ± 18.43	0.002	0.707
CT values of surrounding normal lung tissue (HU)	−874.01 ± 37.82	−867.76 ± 37.62	0.003	0.592
SD values of surrounding normal lung tissue (HU)	27.50 ± 13.71	26.52 ± 9.72	0.183	0.263

CNR, contrast-to-noise ratio;HU, Hounsfield unit; SD, standard deviation; SNR, signal-to-noise ratio.

Table 5. Comparison of subjective scores of the overall image quality of all pulmonary nodules between the two scanning modes

	Score		
	Morphological display of nodules	Visibility for surrounding lung tissue	Artifacts and diagnostic confidence
Standard-dose scan	4.58 ± 0.51	4.51 ± 0.22	4.63 ± 0.82
Low-dose scan	4.52 ± 0.39	4.47 ± 0.36	4.60 ± 0.29
Z value	−0.438	−0.391	−0.416
p value	0.673	0.729	0.694

an area where the density of nodules was uniform, avoiding the edge and necrotic area of nodules, and an area without pathological changes of lung tissue. The CT values and standard deviation (SD) values within the ROI were measured. All data were measured three times and the average values were taken as the final statistical results. The signal-to-noise ratio (SNR) and contrast-to-noise ratio (CNR) of the nodules were calculated using the following formula: $SNR = CT_{nodule} / SD_{nodule}$, $CNR=(CT_{nodule} - CT_{lung\ tissue}) / SD_{lung\ tissue}$, The volumetric CT dose index, dose–length product (DLP) of each patient in the two scan modes were recorded, and the effective dose (ED) calculated as follows: ED = DLP×K ($K = 0.014$).[11] Specifically, the standard-dose scan for the whole lung tissue was recorded as ED_1, the low-dose target scan for pulmonary nodules was recorded as ED_2. In addition, we also recorded the virtual low-dose scan for the whole lung tissue as $ED_{virtual}$ using 24 as a reference noise index, but no actual scans were performed in practice. The scan range of the virtual low-dose scan would be the same as that of standard-dose scan to cover the entire lungs.

Subjective image quality analysis

All reconstructed images were transmitted to an AW4.6 workstation. Two radiologists with more than 10 years of working experience evaluated the subjective image quality using a 5-point scoring system from the aspects of the morphological display of all pulmonary nodules, visibility of surrounding lung tissue, image artifacts and diagnostic confidence in the two scan modes. The specific scoring criteria are listed in Table 1. In addition, partial pulmonary nodules with special morphological signs (lobular sign, burr sign, pleural traction sign and vacuole sign) were also evaluated subjectively by a 5-point method, as detailed in Table 2. The basic information and image parameters of the patients were hidden before evaluation. When the evaluation was inconsistent, the final score was decided by two radiologists after consulting each other.

Statistical analysis

All data were analyzed by SPSS® v. 19.0 (IBM Corp, New York, NY; formerly SPSS Inc, Chicago, IL). For quantitative data, the form of mean ± SD was used to show all the results. The objective parameters (including image noise, SNR and CNR) were compared using the paired-samples *t* test. Subjective scores for the morphological display of pulmonary nodules, visibility of surrounding lung tissue, image artifacts and diagnostic confidence were analyzed using the Mann–Whitney *U* test. A *p*-value of less than 0.05 was considered statistically significant. Cohen's κ test was used to evaluate the interobserver agreements of image quality scores between the two radiologists. Agreements were analyzed as follows: (1) k value of 0–0.20, poor agreement; (2) k value of 0.21–0.40, fair agreement; (3) k value of 0.41–0.60,

Figure 1. Transverse chest CT images of a 62-year-old female with a solid pulmonary nodule in the upper lobe of the right lung. The edges of nodules (arrows) of images reconstructed with FBP in the standard-dose scan (A1) and 60% ASIR-V in the low-dose scan (A2) were all clearly. The scores of the visibility of nodules of FBP image (A1) and 60% ASIR-V image (A2) were 5, 5, respectively. ASIR-V, adaptive statistical iterative reconstruction V; FBP, filtered back projection.

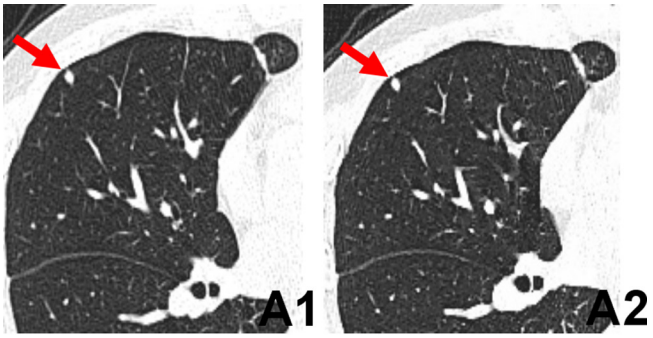

Figure 2. Transverse chest CT images of a 54-year-old male with a mixed-density pulmonary nodule in the middle lobe of the right lung. The edges of nodules (arrows) of images reconstructed with FBP in the standard-dose scan (B1) and 60% ASIR-V in the low-dose scan (B2) appeared blurred. The scores of the visibility of nodules of FBP image (B1) and 60% ASIR-V image (B2) were 3, 3, respectively. ASIR-V, adaptive statistical iterative reconstruction V; FBP, filtered back projection.

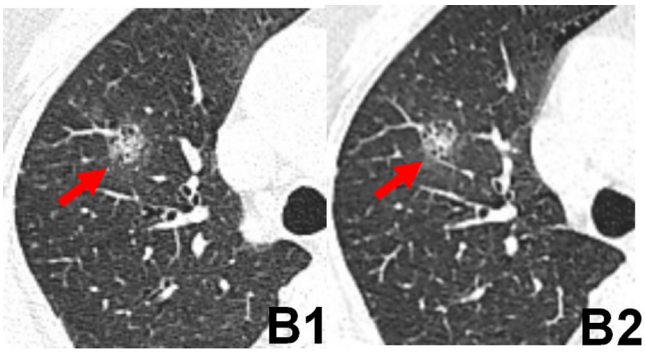

Figure 3. Transverse chest CT images of a 67-year-old male with a solid pulmonary nodule in the lower lobe of the right lung. Both the image reconstructed with FBP in the standard-dose scan (C1) and image reconstructed with 60%ASIR-V in the low-dose scan (C2) clearly showed the vocule sign (green arrows) inside the nodules and the halo sign (red arrows) around the nodules. The scores of the visibility of nodules of FBP image (C1) and 60% ASIR-V image (C2) were 4, 4, respectively. ASIR-V, adaptive statistical iterative reconstruction V; FBP, filtered back projection.

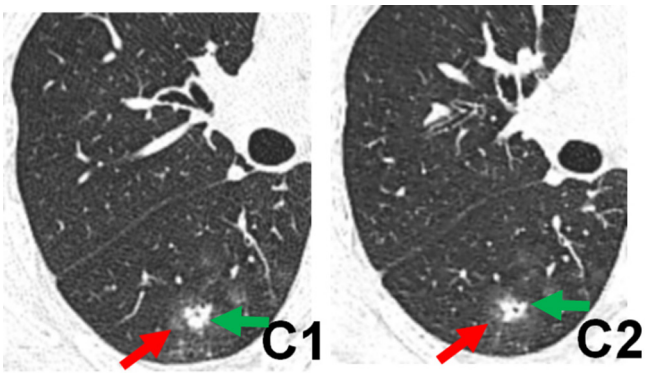

Figure 4. Transverse chest CT images of a 49-year-old female with a ground-glass pulmonary nodule in the lower lobe of the right lung. The edges of nodules (arrows) of images reconstructed with FBP in the standard-dose scan (D1) and 60% ASIR-V in the low-dose scan (D2) appeared blurred. The scores of the visibility of nodules of FBP image (D1) and 60% ASIR-V image (D2) were 3, 3, respectively. However, the other small ground-glass nodule was shown in the lower lobe of the right lung (D1, red solid circle), which was not clearly visible on the same level (D2, red dashed circle). ASIR-V, adaptive statistical iterative reconstruction V; FBP, filtered back projection.

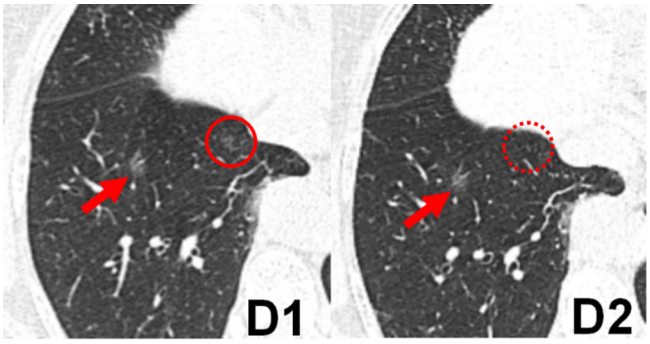

moderate agreement; (4) k value of 0.61–0.80, good agreement; (5) k value of 0.81–1.00, almost excellent agreement.

RESULTS

Objective measurement

A total of 87 pulmonary nodules were detected in the standard-dose scan, and 85 pulmonary nodules were detected in the low-dose scan. Among them, the detection rate of the ground-glass density nodule, mixed-density nodule and solid nodule under the low-dose scanning conditions were 85.71%, 100%, 100%, respectively (Table 3).

The size of pulmonary nodules (the longest diameter, the shortest diameter, and the average diameters), the CT values, SD values, SNR values, CNR values of pulmonary nodules as well as the CT values and SD values of surrounding normal lung tissue had no statistically significant difference between the two scanning modes (Table 4).

Subjective measurement

The two radiologists had good consistencies for the subjective evaluation of the morphological display of nodules ($\kappa = 0.791$, $p < 0.001$), visibility for surrounding lung tissue ($\kappa = 0.826$, $p < 0.001$), artifacts and diagnostic confidence ($\kappa = 0.803$, $p < 0.001$). The subjective image quality scores of the two scan are listed in Table 5. There were no statistically significant differences between the standard-dose scan and low-dose scan in scores for the morphological display of nodules, visibility for surrounding lung tissue, artifacts and diagnostic confidence (Figures 1–4).

As for some pulmonary nodules with special morphologic signs, there were also no statistically significant differences in the subjective scores from the aspects of the lobular sign, burr or spinous, pleural traction sign, vacuoles or voids between the two scanning modes (Table 6).

Effective dose

The volumetricCT dose index and effective dose (ED_1) for the standard-dose scan covering the entire lungs were 7.29 ± 2.38 mGy and 3.52 ± 1.09 mSv, respectively, and those of the low-dose scan targeting pulmonary nodules were 2.56 ± 1.87 mGy and 0.51 ± 0.32 mSv. However, using the low dose scan settings to cover the entire lungs would require an effective dose ($ED_{virtual}$) of 1.44 ± 0.15 mSv, which would mean a dose reduction of 59.1% compared with the standard-dose scan (Table 7).

DISCUSSION

With the continuous development of CT imaging technology, various methods used in pulmonary nodule examination are constantly being updated. The high sensitivity of CT examination makes it a main recommend review method to observe the dynamic changes of pulmonary nodules.[12] The doubling rate of nodules is often used to identify the benign or malignant solitary pulmonary nodules, and it provides a guarantee for the detection of pulmonary nodules and the late follow-up review.[13] However, patients will inevitably receive more radiation during the multiple reviews. Therefore, how to achieve diagnostic chest CT images at low radiation dose to minimize the dose of the entire tested population has become a major public demand for the CT scan.

In recent years, many scholars at home and abroad have done a lot of experiments on how to reduce the radiation dose under the premise of ensuring the image quality and diagnostic accuracy. However, their main research focuses on reducing the tube current.[14] In the CT examination performed for the review of

Table 6. Comparison of subjective scores of the morphological characteristics of partial pulmonary nodules between the two scanning modes

The morphological characteristics	Standard-dose scan Score (5/4/3/2/1)	Low-dose scan Score (5/4/3/2/1)	Z value	*p* value
Lobular sign	11/17/5/0/0	11/15/7/0/0	−0.329	0.715
Burr or spinous	10/14/5/0/0	9/13/7/0/0	−0.494	0.664
Pleural traction sign	9/11/3/0/0	9/10/4/0/0	−0.119	0.793
Vacuole or void	4/5/3/0/0	3/5/4/0/0	−0.590	0.627

specific pulmonary nodules, the imaging physicians usually have certain requirements for the spatial resolution of the image, which is mainly related to the layer thickness, the field of view and the image reconstruction algorithm, and all these factors provide an objective basis for reducing the radiation dose of patients. Due to the large differences in the brand, model and parameters of CT machines used by different medical institutions, the low-dose scanning protocol of various medical institutions are also different, and one of the most important influencing factors is the iterative reconstruction algorithm. Iterative reconstruction algorithms such as iDose4 and IMR by Philips, SAFIRE by Siemens, AIDR-3D by Toshiba as well as ASIR-V and MBIR by GE Healthcare have been proposed in recent years and have achieve certain degrees of dose reduction in clinical appication.[15–18]

Although the traditional FBP reconstruction algorithm is computationally fast, it imposes high requirements on the radiation dose, and it needs the accurate and complete data of each measurement. Meanwhile, the inherent noise of the image will significantly increase under the low radiation dose condition. So, reducing radiation dose is not conducive to further improve the image quality.[19] As the first-generation iterative reconstruction algorithm, ASIR has been widely used in clinical practice. ASIR technique can help to reconstruct high quality image with low noise. MBIR is a more advanced iterative algorithm than ASIR. MBIR has many complex models, including system noise model, object model, physics model and optical model, which all can reduce the image noise more effectively than ASIR. Recent study also suggests that MBIR allows dramatic reduction of radiation dose without affecting image quality and has the potential to further increase the detection rate of some subtle lesions at the expense of longer reconstruction time.[20] As an advanced iterative reconstruction algorithm, ASIR-V is a new reconstruction algorithm between ASIR and MBIR algorithms. ASIR-V reconstruction algorithm takes full account of the digital statistical noise of the data, which helps to better deal with the image artifacts caused by electronic noise and other physical factors. ASIR-V can reduce image noise with a much shorter reconstruction time than MBIR and improve the image quality without seriously degrading the resolution and contrast of all images under low radiation dose conditions.[21,22]

In our study, through the analysis of the objective parameters of pulmonary nodules in the two scanning modes, the results showed that there was no significant difference in the detection of pulmonary nodules, especially for mixed-density nodules and solid nodules. The detection rate of mixed-density nodules and solid nodules in the low-dose scan combined with ASIR-V algorithm was 100%, and that of ground glass nodules was as high as 85%. Two cases of ground-glass density nodules with diameters less than 1 cm were not detected in the low-dose scan group which may indicate the limitation of low-dose CT scans for the detection of lung lesions with low density and small size. Whether optimizing the weighting factors of ASIR-V or using the more sophisticated MBIR algorithms can improve the detection rate in this situation needs further study. On the other hand, the images in low-dose scan did not affect the detection of mixed-density nodules and solid nodules, which was of high sensitivity and could meet the clinical requirements for the follow up of pulmonary nodules. In terms of the size of the lesion, there was not statistically significant difference between the two scanning modes, indicating that the low-dose scan combined with ASIR-V algorithm is still accurate for the measurement of nodules. At the same time, there was no statistical difference in the objective noise, SNR and CNR of nodules in both scan modes, which fully demonstrated that ASIR-V algorithm had strong ability to reduce image noise and provided a theoretical and technical support for the low-dose CT examination.

Table 7. Comparison of radiation dose in the two scanning modes

Parameters	Standard-dose scan For entire lungs	Low-dose scan Targeted scan for nodules	Low-dose scan Virtual scan for entire lungs	*F* value	*p* value
$CTDI_{vol}$ (mGy)	7.29 ± 2.38	2.56 ± 1.87	3.01 ± 0.30	32.056	$p < 0.001$
DLP (mGy·cm)	251.43 ± 77.52	34.83 ± 22.78	102.78 ± 11.04	115.261	$p < 0.001$
ED (mSv)	3.52 ± 1.09	0.51 ± 0.32	1.44 ± 0.15	113.893	$p < 0.001$

$CTDI_{vol}$, volumetric CT dose index; DLP, dose–length product; ED, effective dose.
Virtual scan: only record the radiation dose according to the positioning data, no scans in the actual operation.

In the subjective evaluation in terms of the changes of the internal features of the pulmonary nodules and the surrounding morphology, low-dose CT scan combined with ASIR-V to some extent compensated for the low dose-induced higher image noise, making low-dose CT images to have the same quality as standard-dose scans, and the image quality fully meets the clinical diagnosis requirements. In addition, due to the high air content in lungs, there is a good natural contrast between the pulmonary nodules and lung tissue, which is not affected by the image noise fluctuation. It is precisely because of the high contrast between the pulmonary nodules and lung tissue, within a certain range, the increase of image noise has little effect on the detailed display and observation of pulmonary nodules.

In terms of radiation dose, the results of our study showed that the virtual effective dose of low-dose chest CT scan to cover the entire lungs could be 1.44 ± 0.15 mSv. This was a reduction of about 59.1% compared with the 3.52 ± 1.09 mSv in the standard-dose scan. This is especially important for patients who need early lung cancer screening, or for patients who need regular follow-up CT examinations for dynamic changes of the lesion. Therefore, low-dose CT scan can significantly reduce the cumulative radiation dose of patients and has important clinical significance.[23,24]

There were several limitations in our present study. First, our study focused on detection rate instead of diagnostic accuracy, the potential false positive rates were not evaluated in the present study. Second, our study focused on the display of morphological features of the pulmonary nodule. However, low-dose CT scans may impact on the observation of mediastinal structures. Even though the observation requirements for mediastinal structures were not as high in the detection and follow-up review of pulmonary nodules, its impact needs to be further studied. Third, although the two experienced radiologists had used blind methods to evaluate the image quality without patient basic information on the images, there still existed some subjective bias for the data characteristics of the two reconstruction algorithms. In addition, the detection rate for the low-dose scan with ASIR-V may also be favorably biased by two facts: (a) all images that were evaluated in the low-dose study had nodules. Therefore, readers knew they had to find at least one nodule in the low-dose scan and, most likely, were looking closer and longer than they would in clinical routine; (b) the targeted scans had much smaller scan range. Hence, readers had to analyze smaller fields of interests than in clinical routine. Finally, the sample size was not large enough, we have only studied a very small number of people, and we need to do more with a large sample.

CONCLUSION

The low-dose CT scan combined with ASIR-V algorithm is of comparable value in the detection of pulmonary nodules and the display of the morphological signs of nodules when compared with the images obtained by standard-dose scan. Low-dose scan can significantly reduce the radiation dose and is recommended for primary screening and follow-up for pulmonary nodules.

REFERENCES

1. Carr SR, Schuchert MJ, Pennathur A, Wilson DO, Siegfried JM, Luketich JD, et al. Impact of tumor size on outcomes after anatomic lung resection for stage 1A non-small cell lung cancer based on the current staging system. *J Thorac Cardiovasc Surg* 2012; **143**: 390–7. doi: https://doi.org/10.1016/j.jtcvs.2011.10.023
2. Yoon HJ, Chung MJ, Hwang HS, Moon JW, Lee KS. Adaptive statistical iterative Reconstruction-Applied Ultra-Low-Dose CT with Radiography-Comparable radiation dose: usefulness for lung nodule detection. *Korean J Radiol* 2015; **16**: 1132–41. doi: https://doi.org/10.3348/kjr.2015.16.5.1132
3. Brenner DJ, Hall EJ. Computed tomography--an increasing source of radiation exposure. *N Engl J Med* 2007; **357**: 2277–84. doi: https://doi.org/10.1056/NEJMra072149
4. Rusinek H, Naidich DP, McGuinness G, Leitman BS, McCauley DI, Krinsky GA, et al. Pulmonary nodule detection: low-dose versus conventional CT. *Radiology* 1998; **209**: 243–9. doi: https://doi.org/10.1148/radiology.209.1.9769838
5. Aberle DR, Adams AM, Berg CD, Black WC, Clapp JD, Fagerstrom RM, et al. Reduced lung-cancer mortality with low-dose computed tomographic screening. *N Engl J Med* 2011; **365**: 395–409. doi: https://doi.org/10.1056/NEJMoa1102873
6. Kligerman S, Mehta D, Farnadesh M, Jeudy J, Olsen K, White C, et al. Use of a hybrid iterative reconstruction technique to reduce image noise and improve image quality in obese patients undergoing computed tomographic pulmonary angiography. *J Thorac Imaging* 2013; **28**: 49–59. doi: https://doi.org/10.1097/RTI.0b013e31825412b2
7. Tang H, Yu N, Jia Y, Yu Y, Duan H, Han D, et al. Assessment of noise reduction potential and image quality improvement of a new generation adaptive statistical iterative reconstruction (ASIR-V) in chest CT. *Br J Radiol* 2018; **91**: 20170521. doi: https://doi.org/10.1259/bjr.20170521
8. Benz DC, Gräni C, Mikulicic F, Vontobel J, Fuchs TA, Possner M, et al. Adaptive statistical iterative reconstruction-V: impact on image quality in ultralow-dose coronary computed tomography angiography. *J Comput Assist Tomogr* 2016; **40**: 958–63. doi: https://doi.org/10.1097/RCT.0000000000000460
9. De Marco P, Origgi D. New adaptive statistical iterative reconstruction ASiR-V: assessment of noise performance in comparison to ASiR. *J Appl Clin Med Phys* 2018; **19**: 275–86. doi: https://doi.org/10.1002/acm2.12253
10. Kwon H, Cho J, Oh J, Kim D, Cho J, Kim S, et al. The adaptive statistical iterative reconstruction-V technique for radiation dose reduction in abdominal CT: comparison with the adaptive statistical iterative reconstruction technique. *Br J Radiol* 2015; **88**: 20150463. doi: https://doi.org/10.1259/bjr.20150463
11. Huda W, Ogden KM, Khorasani MR. Converting dose-length product to effective dose at CT. *Radiology* 2008; **248**: 995–1003. doi: https://doi.org/10.1148/radiol.2483071964
12. Xie X, Heuvelmans MA, van Ooijen PMA, Oudkerk M, Vliegenthart R. A practical approach to radiological evaluation of CT lung cancer screening examinations. *Cancer*

Imaging 2013; **13**: 391–9. doi: https://doi.org/10.1102/1470-7330.2013.9043
13. Berbaum KS, Schartz KM, Caldwell RT, Madsen MT, Thompson BH, Mullan BF, et al. Satisfaction of search from detection of pulmonary nodules in computed tomography of the chest. *Acad Radiol* 2013; **20**: 194–201. doi: https://doi.org/10.1016/j.acra.2012.08.017
14. Kalra MK, Rizzo S, Maher MM, Halpern EF, Toth TL, Shepard J-AO, et al. Chest CT performed with z-axis modulation: scanning protocol and radiation dose. *Radiology* 2005; **237**: 303–8. doi: https://doi.org/10.1148/radiol.2371041227
15. Laqmani A, Kurfürst M, Butscheidt S, Sehner S, Schmidt-Holtz J, Behzadi C, et al. Ct pulmonary angiography at reduced radiation exposure and contrast material volume using iterative model reconstruction and iDose4 technique in comparison to FBP. *PLoS One* 2016; **11**: e0162429. doi: https://doi.org/10.1371/journal.pone.0162429
16. Scharf M, Brendel S, Melzer K, Hentschke C, May M, Uder M, et al. Image quality, diagnostic accuracy, and potential for radiation dose reduction in thoracoabdominal CT, using Sinogram Affirmed iterative reconstruction (SAFIRE) technique in a longitudinal study. *PLoS One* 2017; **12**: e0180302. doi: https://doi.org/10.1371/journal.pone.0180302
17. Mirsadraee S, Weir NW, Connolly S, Murchison JT, Reid JH, Hirani N, et al. Feasibility of radiation dose reduction using AIDR-3D in dynamic pulmonary CT perfusion. *Clin Radiol* 2015; **70**: 844–51. doi: https://doi.org/10.1016/j.crad.2015.04.004
18. Park C, Choo KS, Kim JH, Nam KJ, Lee JW, Kim JY, et al. Image quality and radiation dose in CT venography using model-based iterative reconstruction at 80 kVp versus adaptive statistical iterative Reconstruction-V at 70 kVp. *Korean J Radiol* 2019; **20**: 1167–75. doi: https://doi.org/10.3348/kjr.2018.0897
19. Kuo Y, Lin Y-Y, Lee R-C, Lin C-J, Chiou Y-Y, Guo W-Y, et al. Comparison of image quality from filtered back projection, statistical iterative reconstruction, and model-based iterative reconstruction algorithms in abdominal computed tomography. *Medicine* 2016; **95**: e4456. doi: https://doi.org/10.1097/MD.0000000000004456
20. Benz DC, Fuchs TA, Gräni C, Studer Bruengger AA, Clerc OF, Mikulicic F, et al. Head-To-Head comparison of adaptive statistical and model-based iterative reconstruction algorithms for submillisievert coronary CT angiography. *Eur Heart J Cardiovasc Imaging* 2018; **19**: 193–8. doi: https://doi.org/10.1093/ehjci/jex008
21. Lim K, Kwon H, Cho J, Oh J, Yoon S, Kang M, et al. Initial phantom study comparing image quality in computed tomography using adaptive statistical iterative reconstruction and new adaptive statistical iterative reconstruction V. *J Comput Assist Tomogr* 2015; **39**: 1–8. doi: https://doi.org/10.1097/RCT.0000000000000216
22. Lee J. Correction to the adaptive statistical iterative reconstruction-V technique for radiation dose reduction in abdominal CT: comparison with the adaptive statistical iterative reconstruction technique. *Br J Radiol* 2016; **89**: 20150463e. doi: https://doi.org/10.1259/bjr.20150463.e
23. Ono K, Hiraoka T, Ono A, Komatsu E, Shigenaga T, Takaki H, et al. Low-Dose CT scan screening for lung cancer: comparison of images and radiation doses between low-dose CT and follow-up standard diagnostic CT. *Springerplus* 2013; **2**: 1–8. doi: https://doi.org/10.1186/2193-1801-2-393
24. Tartari S, Rizzati R, Righi R, Deledda A, Terrani S, Benea G, et al. Low-Dose unenhanced CT protocols according to individual body size for evaluating suspected renal colic: cumulative radiation exposures. *Radiol Med* 2010; **115**: 105–14. doi: https://doi.org/10.1007/s11547-009-0476-5